17600

NATIONAL LIBRARY
OTTAWA

CANADA

BIBLIOTHÈQUE NATIONALE
OTTAWA

NAME OF AUTHOR... ROBERT HUGH MCCAMIS

TITLE OF THESIS... THE TOTAL CROSS SECTIONS OF THE REACTIONS $^{16}O(p,ALPHA)^{13}N$ AND $^{10}B(ALPHA,N)^{13}N$

UNIVERSITY... ALBERTA

DEGREE FOR WHICH THESIS WAS PRESENTED... M. Sc.

YEAR THIS DEGREE GRANTED... 1973

Permission is hereby granted to THE NATIONAL LIBRARY OF CANADA to microfilm this thesis and to lend or sell copies of the film.

The author reserves other publication rights, and neither the thesis nor extensive extracts from it may be printed or otherwise reproduced without the author's written permission.

(Signed)... R.H. McCamis

PERMANENT ADDRESS:

DEPT. OF PHYSICS
UNIVERSITY OF ALBERTA
EDMONTON

DATED... OCTOBER 2 ... 1973.

NL-91 (10-68)

THE UNIVERSITY OF ALBERTA

THE TOTAL CROSS SECTIONS OF THE REACTIONS ^{16}O (p, alpha) ^{13}N AND ^{10}B (alpha, n) ^{13}N

by

(C)

ROBERT HUGH McCAMIS

A THESIS

SUBMITTED TO THE FACULTY OF GRADUATE STUDIES AND RESEARCH IN

PARTIAL FULFILMENT OF THE REQUIREMENTS FOR THE DEGREE OF

MASTER OF SCIENCE

in

NUCLEAR PHYSICS

DEPARTMENT OF PHYSICS

EDMONTON, ALBERTA

FALL, 1973

THE UNIVERSITY OF ALBERTA

FACULTY OF GRADUATE STUDIES AND RESEARCH

The undersigned certify that they have read, and recommend to the Faculty of Graduate Studies and Research for acceptance, a thesis entitled "The Total Cross Sections of the Reactions ^{16}O (p, alpha) ^{13}N and ^{10}B (alpha, n) ^{13}N," submitted by Robert Hugh McCamis in partial fulfilment of the requirements for the degree of Master of Science in Nuclear Physics.

G. A. Moss
.....
Dr. G. A. Moss, Supervisor

John M Cameron
.....
Dr. J. M. Cameron

J. A. Kernahan
.....
Dr. J. A. Kernahan

F. E. Vermeulen
.....
Dr. F.E. Vermeulen

Date September 13, 1973

ABSTRACT

The reaction $^{16}O(p,\alpha)\ ^{13}N$ plays an important part in explosive oxygen and silicon burning phases in stars, and the magnitude of its cross section is thus important in various astrophysical models of stellar evolution. Therefore, this reaction cross section was measured over the energy range of astrophysical interest, i.e., from 5.55 MeV (threshold) to 7.7 MeV. The experiment was done using an activation procedure, where a target is bombarded with protons, then removed and the induced activity is measured. At the highest energies obtained, the cross section was compared to, and agrees very well with, some previous measurements. The reaction rate was calculated to be 0.049 cm^3/g-sec, which is significantly lower than the previous estimate of 0.308 cm^3/g-sec.

In addition the cross section of $^{10}B(\alpha,n)\ ^{13}N$ was also found using the activation procedure. The region of astrophysical interest here is below 1.5 MeV. A large resonance is found at 1.545 MeV, in agreement with previous work, and a slight shoulder is seen at 1.33 MeV. A discrepancy in the magnitude of the peak cross section by a factor of 3.5 between the present and previous work is found and discussed. The reaction rate for this reaction is found

to be 1.9×10^4 $cm^3/g\text{-}sec$, as compared to the previous estimate of 57.2×10^4 $cm^3/g\text{-}sec$.

ACKNOWLEDGEMENTS

I am immensely grateful to my supervisor, Dr. G. A. Moss, both for his continual help and guidance during the course of this work, and for imparting countless bits of information that together gave me some idea of what Nuclear Physics is all about.

The aid and encouragement of Dr. J. M. Cameron has also been invaluable, especially at those times when it seemed that the experiments would never work.

I am grateful to Dr. G. C. Neilson for his suggestion of using the MgO_2 targets, which really saved the day. I would also thank Drs. D. Gill and D. Hutcheon for many comments and discussion.

The fact that both accelerators ran so well during my experiments, especially when operated beyond their normal limits, is a reflection of the excellent technical work provided by Lars, Paul, Ron, John H., Pete, Con, Henry, Don, Jan, John R., Earl, and last but by no means least, "Uncle Jock" Elliott of NRC and Ron G. and Fred B. of the Chemistry Radiation Laboratory.

I am also grateful to the 920 and 516 for their help in collecting and analyzing the data, even if, at times, their ideas about what should be done next differed somewhat from mine. I would like to thank Dr. K. Dawson for his expert help

with the computers, and Jim Easton for providing the LSQ fitting program, which was an integral part of this work.

I wish to thank the Department of Chemistry and Dr. G. Freeman for their cooperation in providing me with time on their machine, and the Astrophysics Group of the Physics Department for the loan of the automatic printout system, which helped data collecting very much. The help of P. Pang and K. Wanke in running part of the $^{10}B(\alpha,n)$ work is also appreciated.

The friendship, cooperation and helpful discussion of my fellow graduate students, Woon C., Sayed E., Tilak S., Ed W., Peter G., Jim P., Jan S., Ahmed H., Dave W., Peter J., Barb P., and Steve M. have been a very great help.

I am grateful to Misses Greta Tratt, Audrey Forman and Cheryl Link for their help in so many ways, and for brightening up many a dull day.

My sincerest thanks go to Mrs. M. Wahl and Mrs. B Scott for their excellent typing of this thesis, in spite of many problems and deadlines.

I am very grateful to the University of Alberta and the National Research Council of Canada for their financial assistance during the course of this work.

Many exemplary contributions have been made by people whom space does not permit me to mention. To all of these people, I apologize and I express my appreciation.

Finally, I would like to thank my parents and my brothers for everything they have done for me over the years. Words alone are inadequate to describe my feelings.

TABLE OF CONTENTS

Chapter		Page
I.	INTRODUCTION	1
II.	THE $^{16}O(p,\alpha)\ ^{13}N$ REACTION	4
	2.1 Targets	4
	2.2 Target Thickness Determination	7
	2.3 Activation Procedure	9
	2.4 Counting Arrangement	12
	2.5 Data Analysis	14
	2.6 Results and Discussion	21
III.	THE $^{10}B(\alpha,n)\ ^{13}N$ REACTION	28
	3.1 Accelerators	28
	3.2 Targets	28
	3.3 Target Thickness Determination	29
	3.4 Activation Procedure	29
	3.5 Counting Arrangement	34
	3.6 Data Analysis	38
	3.7 Results and Discussion	40
IV.	CONCLUSIONS	46
REFERENCES		48
APPENDICES:	A RELEVANT ASTROPHYSICAL THEORY	52
	B CROSS SECTION CALCULATION	56

LIST OF FIGURES

Figure		Page
1.	Schematic Beam Line Configuration	8
2.	Proton Spectrum From MgO_2 Target at 165°	10
3.	The Plexiglass NaI Counting Stand (Not to Scale)	13
4.	Efficiency of NaI Versus Gamma Ray Energy	15
5.	Spectrum for NaI Showing 0.511 MeV Peak	16
6.	Dead Time of System Versus Count-Rate	18
7.	Decay Curve for Activated Oxygen Target	19
8.	Total Cross Section of $^{16}O(p,\alpha)\ ^{13}N$ With Penetration Function	25
9.	Schematic Beam Line Configuration at the Chemistry Radiation Laboratory	30
10.	Enlarged View of Target Box	32
11.	Beam Averaging RC Circuit	33
12.	Coincidence NaI Counting Stand (Not to Scale)	36
13.	Schematic Coincidence Electronics Diagram	37
14.	Decay Curve For Activated Boron Target	39
15.	Total Cross Section of $^{10}B(\alpha,n)$ Versus Energy	41
16.	Sketch of the Gamow Peak	55

LIST OF TABLES

Table		Page
1.	CROSS SECTION vs. ENERGY FOR $^{16}O(p,\alpha)\ ^{13}N$	24
2.	$^{10}B(\alpha,n)\ ^{13}N$ CROSS SECTION vs. ENERGY	42

CHAPTER I

INTRODUCTION

In recent years, astrophysicists have formulated several theories and models of stellar interiors and stellar evolution. The calculations of stellar evolution require the reaction rate of every nuclear reaction that is possible among the nuclei composing a star. In the past, some of the reaction rates used were theoretical or semitheoretical predictions and were often incorrect by orders of magnitude. These predictions can be tested using the experimental cross sections for the reactions in a pertinent energy region. However, there still exist a great many nuclear reactions whose cross sections are important to varying degrees, but have not, as yet, been experimentally determined in the important energy region.

One of the more important of these reactions is the reaction $^{16}O(p,\alpha)^{13}N$. This reaction is important during carbon, oxygen, and silicon burning phases of stellar evolution. A star undergoing explosive oxygen burning has oxygen destroyed by three main modes (Woosley, Arnett and Clayton, 1972):

$$^{16}O + {}^{16}O \rightarrow {}^{28}Si + \alpha \qquad (1)$$

$$^{16}O + \gamma \rightarrow {}^{12}C + \alpha \text{ and}$$

$$^{12}C + {}^{16}O \rightarrow {}^{24}Mg + \alpha \rightarrow {}^{28}Si \quad (2)$$

$$^{16}O\ (\gamma,\alpha)\ {}^{12}C(^{12}C,\alpha)\ {}^{20}Ne\ (\gamma,\alpha)\ {}^{16}O \quad (3)$$

which is equivalent to

$$^{16}O + {}^{16}O \rightarrow {}^{16}O + 4\alpha.$$

Each of these modes dominates at a different temperature and density, and various combinations of modes 1, 2, and 3 result in different relative abundances of nuclei with $30 \leq A \leq 40$. However, a fourth mode of oxygen burning which was suggested to be important under certain conditions is:

$$^{16}O\ (p,\alpha)\ {}^{13}N\ (\gamma,p)\ {}^{12}C \quad (4)$$

as pointed out by Woosley et al. (Woosley et al., 1972). This is similar to mode 2 above, and, depending on the reaction rate involved, can have sizeable effects on relative abundances.

It has also been shown (Woosley, 1973 and Bodansky, Clayton and Fowler, 1968) that under certain conditions (chiefly very high temperatures) the $^{16}O\ (\gamma,\alpha)\ {}^{12}C$ reaction rate controls the rate of silicon burning. Mode 4 can obviously contribute to this reaction especially for stars which have, at this stage in their evolution, a high proton density. In fact, it has been shown (Woosley, 1973 and Woosley, Arnett and Clayton, 1973) that the (p,α) chain can even dominate the (γ,α) reaction in destroying oxygen for certain densities and temperatures.

The importance of oxygen burning reactions during hydrostatic carbon burning has also been demonstrated (Arnett and Truran, 1969).

The only previous value for the reaction rate of ^{16}O (p,α) ^{13}N was derived from a semiempirical formula of Wagoner (Wagoner, 1969) which could possibly have been high by an order of magnitude.

Therefore, it was decided to measure the cross section for this reaction in the important energy range, 5.55 MeV (the reaction threshold) to 7.5 MeV, using an activation procedure. This was done not only because of the astrophysical reasons above, but also because it was a cross section which had not been measured. The activation method, whereby a target is exposed to a beam of particles and then removed and examined for any induced activity, was chosen because the ^{13}N, which is β^+ unstable with a half-life of 10.0 minutes, was very amenable to this technique.

It was also decided to measure the $^{10}B(\alpha,n)\ ^{13}N$ reaction cross section because it could be measured using essentially the same procedure and it would be another test of the validity of Wagoner's estimates.

The results of these two measurements are given in the remainder of this thesis. Chapter II discusses the ^{16}O (p,α) ^{13}N experiment, and Chapter III contains the $^{10}B(\alpha,n)\ ^{13}N$ experiments. The conclusions of the present work are summarized in Chapter IV.

CHAPTER II

THE ^{16}O (p,α) ^{13}N REACTION

2.1 Targets

The first and most important part of any nuclear physics experiment is the preparation of suitable targets. The chief requirements of the ^{16}O targets used in this experiment were physical strength, purity, reasonable thickness, and the minimization of the presence of any nuclei which had reactions possible leading to β^+ unstable nuclei with half-lives between one minute and two hours. A number of target materials and a variety of preparation procedures were tried before the final targets were selected.

The first targets tried were self-supporting SiO_2 films, the making of which has been described before (Sharma, 1972). These targets were unsatisfactory for several reasons. They were physically weak, and, because of the high temperatures (and therefore currents) required to evaporate the SiO_2 powder, were very hard to make. It was also difficult to get targets of sufficient thickness, because of the tendency of thick layers of SiO_2 to crack when inserted into the flotation bath.

Because of the above reasons, these targets were replaced by ones of SiO_2 evaporated directly onto aluminum foils that were approximately 170 $\mu gm/cm^2$ thick. The

aluminum foil was added to give the target strength and also to catch the recoiling ^{13}N nuclei and prevent them from leaving the target. However, in addition to the ^{13}N produced in the primary reaction, and ^{18}F, produced in the unavoidable reaction ^{18}O (p,n) ^{18}F, which has a half-life of 110 minutes, ^{30}P was produced by the reactions $^{29}Si(p,\gamma)$ ^{30}P and $^{30}Si(p,n)$ ^{30}P. ^{30}P is β^+ unstable with a half-life of 2.5 minutes and this drastically masked the amount of ^{13}N that was present after the bombardment, especially in those runs where the amount of ^{13}N was very small. Therefore, the targets made of SiO_2 were set aside.

The next targets tried were vanadium pentoxide (V_2O_5), also evaporated onto the 170 $\mu gm/cm^2$ aluminum foil. One reason for choosing V_2O_5 was the fact that its melting point is 690°C, as opposed to 1700°C for SiO_2, making the V_2O_5 much easier to evaporate. Also, the ratio of 5 oxygen atoms per molecule was helpful.

One part of the purity requirement that was vital was that the targets be as free of carbon as possible. The reactions ^{12}C (p,γ) and ^{13}C (p,n) both give ^{13}N, so that the amount of ^{13}N produced from the principal reaction was masked. Using the number of protons elastically scattered from carbon (see below) and the known elastic scattering differential cross sections from carbon (Swint et al., 1966) attempts were made to determine the amount of carbon present in the targets. Thus, knowing the cross sections for the two carbon reactions (Cohen, 1955) and (Dagley et al., 1961),

respectively, it was possible to calculate the amount of ^{13}N in the target produced from the carbon. However, it was found that the uncertainties introduced by this procedure were sizeable, and attempts were made to produce carbon-free targets.

Targets of Ta_2O_5 and LiO_2 were tried, among others, but it was soon concluded that the high carbon content of the targets came from the evaporation procedure itself, so new methods of making targets were sought.

Next, some magnesium peroxide (MgO_2) targets were made. For these targets, gold leaf approximately 3.3 microns thick was placed on target blanks and used as the backing material. The targets were made by taking a short piece (approximately 2 to 4 inches) of magnesium ribbon and igniting it. A dense, whitish cloud of magnesium peroxide smoke was given off and was allowed to impinge upon the gold backing where the MgO_2 was deposited in a fairly uniform layer. The targets used were approximately 300 to 400 $\mu gm/cm^2$ thick, although this figure could easily be adjusted by adjusting the length of ribbon allowed to burn. The targets thus obtained were reasonably strong and free of contaminants, especially carbon, and were also very quickly and very easily manufactured. The only safety precaution necessary was to ensure that the extremely hot burning magnesium, or its ash, did not fall upon any flammable surface.

2.2 Target Thickness Determination

The targets were activated using the beam line configuration shown in Figure 1. Simultaneously, the thickness of the target was determined by monitoring the protons elastically scattered from the target at laboratory angles of 105° and 165°. The detectors used were silicon surface barrier detectors with thicknesses of 500 and 1000 microns. These detectors were collimated by discs, with a 0.116 inch diameter aperture in them at a position 7 inches from the center of the target, accurately defining the solid angles subtended by the detectors. The signals from these detectors were amplified and fed into analog to digital converters which were connected on-line to the Honeywell DDP-516 computer.

The large angle (165°) spectrum was preferable because protons scattered from nuclei of differing masses in the target were separated kinematically much better than at the smaller angle, and so was used to determine the target thickness wherever possible. However, at certain energies the differential cross section for scattering from ^{16}O at 165° was so small that the smaller angle data had to be used. In order to ensure the correct identification of each major peak in the spectrum, the kinematics for scattering from each nucleus present in the target was obtained for the appropriate energies and angles using a two-body relativistic kinematics computer program. The predicted energies were compared with the energies of the

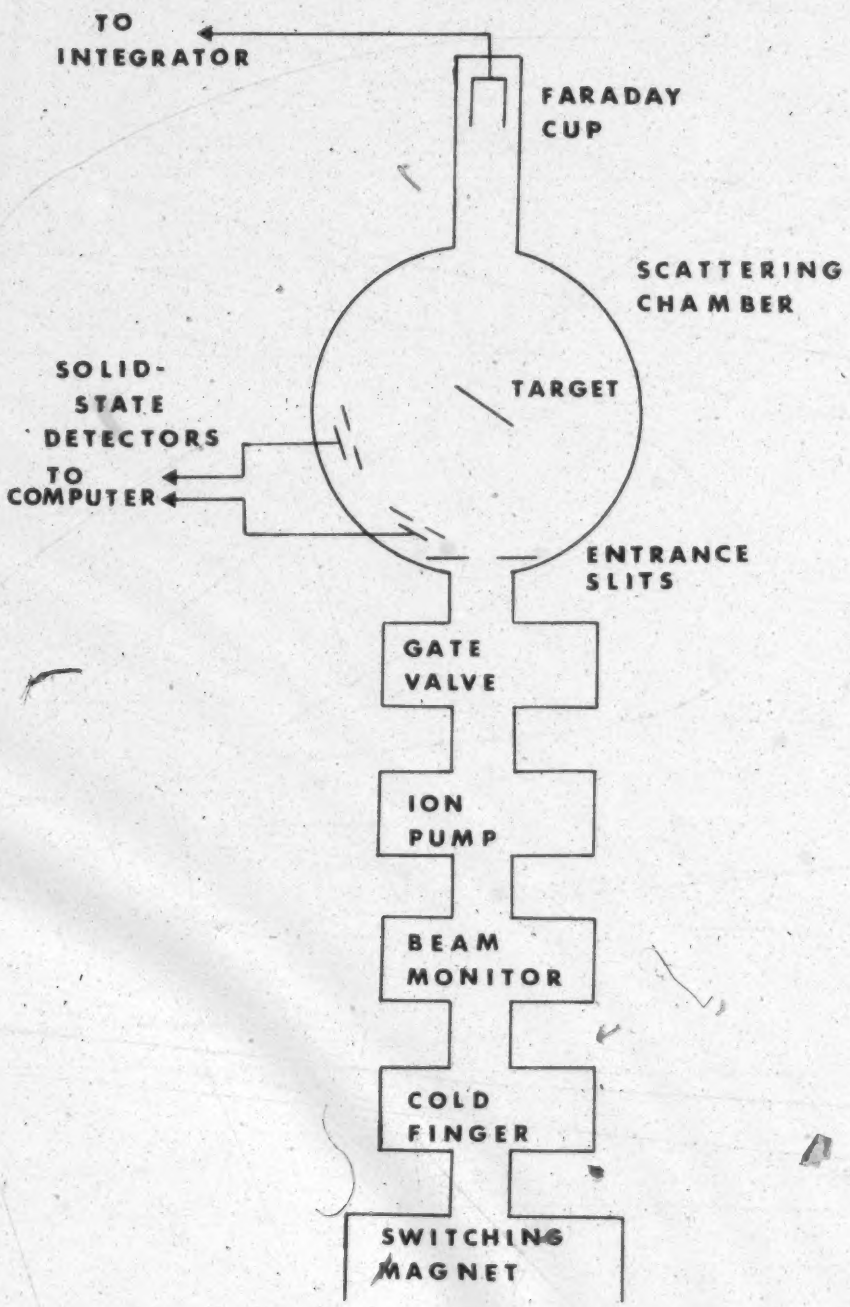

FIGURE 1 SCHEMATIC BEAM LINE CONFIGURATION

peaks obtained by an appropriate energy calibration of the spectrum.

A typical proton spectrum is shown in Figure 2. The major elastic and inelastic peaks are indicated. It should be noted that the spectrum is very clean and the peaks are well separated. It should also be noted that in none of the elastic spectra obtained were there any indications of a ^{14}N elastic peak. This will be discussed later.

Using the differential cross section for ^{16}O (p,p) (Salisbury et al., 1962) the thickness of the target was found as outlined in Appendix B.

The chief advantage in the above procedure was that not only was the target thickness determined, but the identity and also the amounts of the various contaminants were simultaneously obtained. The only quantity needed to determine the amount of any specific impurity was its differential cross section at the particular angle and energy under consideration.

2.3 Activation Procedure

The first requirement for activating a target consisted of obtaining a steady, high intensity beam of protons from the University of Alberta 7.5 MeV CN Van de Graaff Accelerator. The high intensity requirement resulted from the fact that the amount of ^{13}N produced during the activation is directly proportional to the current incident on the target. The steadiness was a demand of the method of

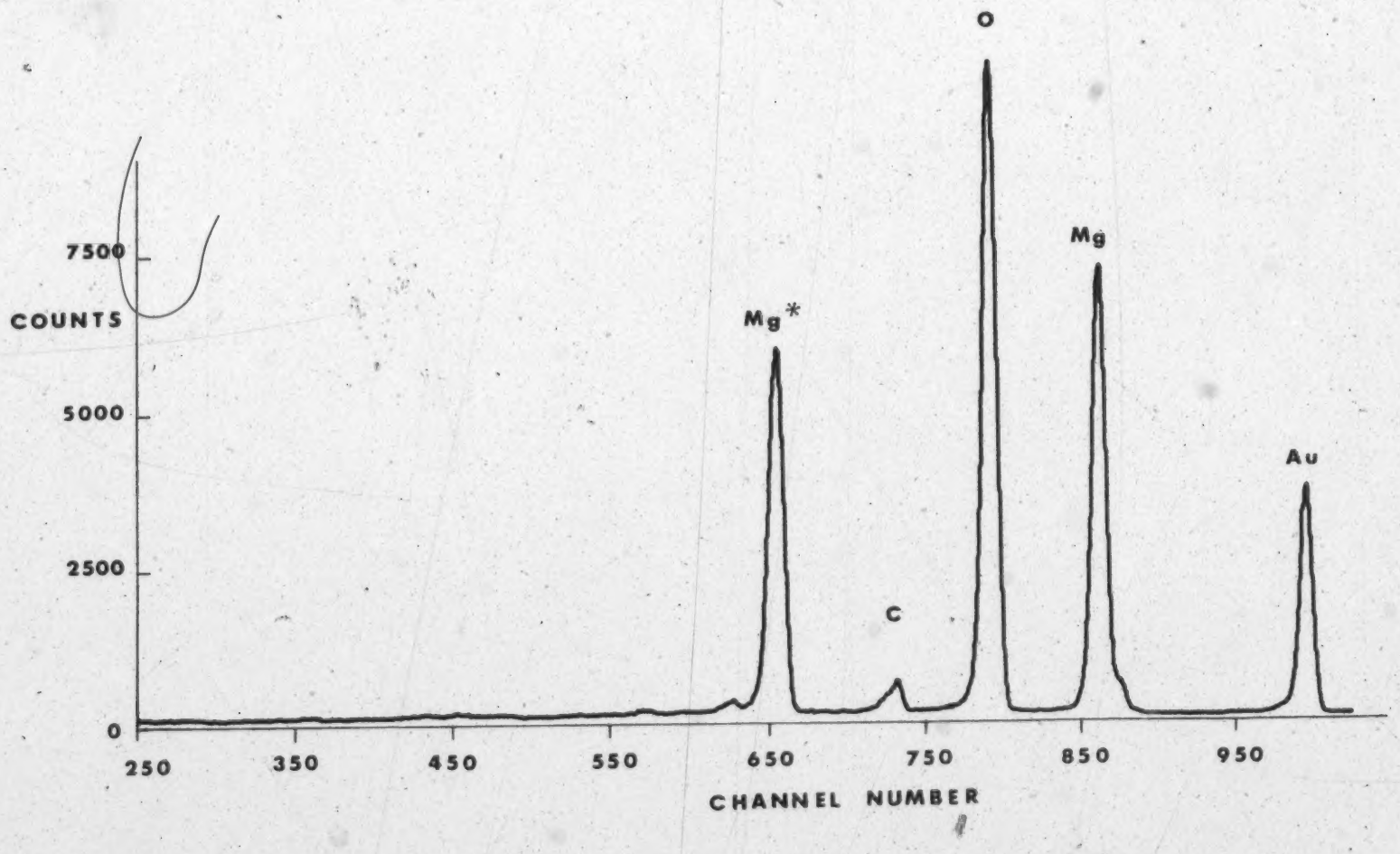

FIGURE 2 PROTON SPECTRUM FROM MgO_2 TARGET AT 165°

analysis, which assumed that the product of the incoming beam current times the number of target nuclei per cm^2 was constant over the period of the activation (see Appendix B). The beam intensity at the target varied from run to run between 0.8 and 1.5 microamperes.

When a suitable beam was obtained, the target was inserted into the beam and left there for a certain time while the elastic scattering data was being taken. The amount of time that the target was left in the beam involved a certain amount of compromise. Allowing the activation to proceed for a longer time produced more ^{13}N, but it also produced more ^{18}F, by ^{18}O (p,n) ^{18}F. The time that most of the targets were bombarded for was 20 minutes, which is two half-lives of ^{13}N. At this point, roughly 75 per cent of the maximum amount (which is reached when the decay rate equals the production rate) of ^{13}N possible was produced, as compared with about 12 per cent of the maximum amount of ^{18}F.

The protons passing through the target were collected in a Faraday cup about two feet downstream and integrated to obtain the total charge incident upon the target. Since this total charge did not enter the calculation of the cross section (see Appendix B), little attention was given to the problem of secondary electron emission from the Faraday cup.

After the target had been bombarded for the required length of time, the beam was stopped, the chamber opened and the target quickly removed to the counting assembly. This procedure normally took from 2 to 3 minutes, the longest

time being taken in venting the scattering chamber to the atmosphere.

2.4 Counting Arrangement

After being activated, the target was placed under a 3" x 3" NaI (Tl) scintillation counter, which was used to detect the 0.511 MeV γ-rays resulting from the annihilation of β^+ particles coming from the residual nuclei. The counter was held in a special plexiglass stand (Figure 3). This stand provided both support for the counter and a reproducible counting geometry with a well-defined solid angle. It was constructed so that the front face of the detector could be moved, in one inch increments, from 6 inches to 15 inches from the target. The base of the stand had shallow indentations in it so that either a calibrated γ-ray source or a target could be positioned directly along the axis of the detector above it. An aluminum annihilator plate was placed over the target to ensure that the β^+'s were annihilated in a well-defined volume, either by the aluminum plate or the base of the stand.

The counting was done with the NaI counter in a room other than the main target room, in an attempt to reduce the background radiation entering the detector. Long background runs taken showed that while a great many γ-rays from long-lived isotopes were present in small amounts, only the 1.460 MeV γ-ray of ^{40}Ar, formed when ^{40}K ($\tau_{1/2}$ = 1.26×10^9 years) decayed, was present to any significant

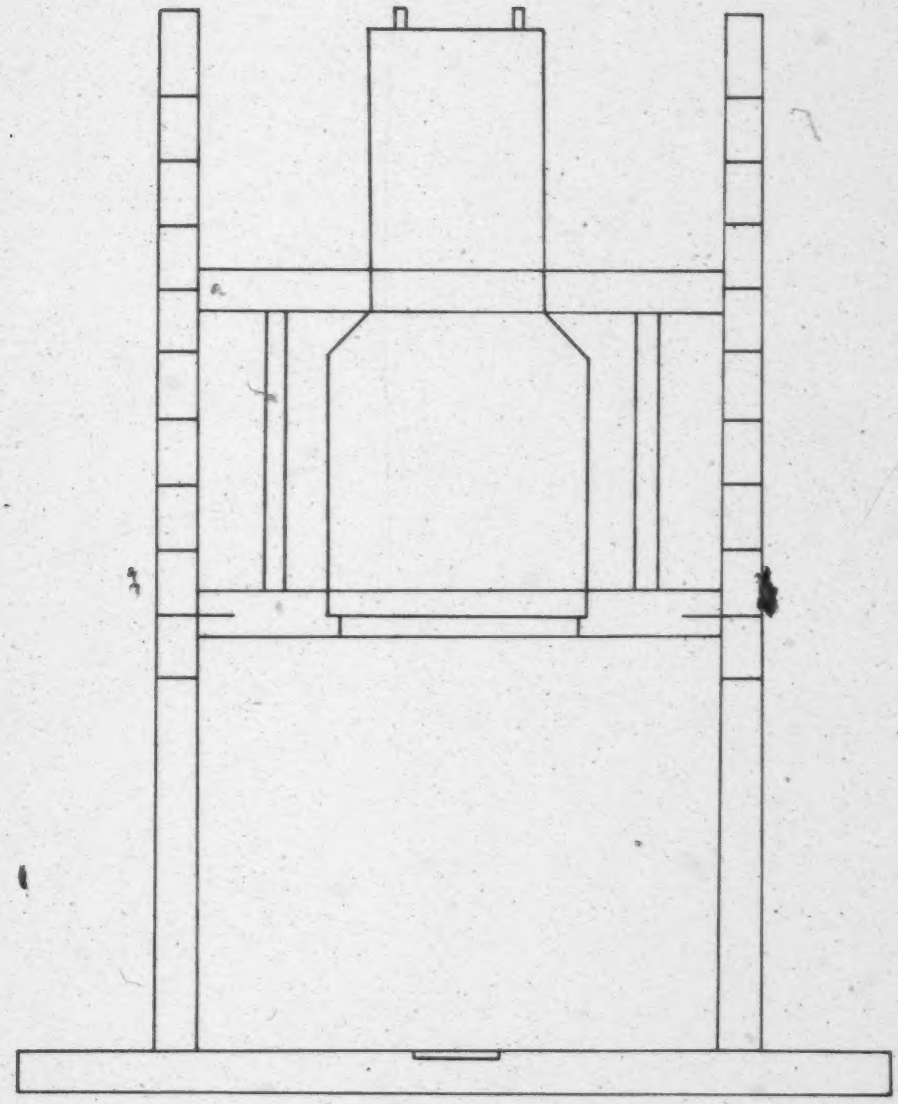

FIGURE 3 THE PLEXIGLASS NaI COUNTING STAND
(NOT TO SCALE)

extent. Since this γ-ray had an energy far removed from that of the annihilation γ-rays it was not a hindrance during the experiments.

The efficiency of the scintillation counter was measured for each position of the counter in the stand as a function of γ-ray energy. Calibrated γ-ray sources were used to provide the 0.511 and 1.280 MeV γ-rays from ^{22}Na, the 0.662 MeV γ-ray from ^{137}Cs, and the 0.835 MeV γ-ray from ^{54}Mn. The results of these measurements are given in Figure 4.

The amplified signals from the counter were sent into the main control room and fed into the DDP-516 or the SDS-920 computer via an analog to digital converter. The data was accumulated for one minute, which resulted in a spectrum similar to Figure 5. The sums of the three regions A, B, and C, shown in Figure 5, were taken. The counting was repeated in this fashion for about 60 to 80 minutes, with the time between counting periods being approximately 20 seconds. By this time, essentially all the 10 minute half-life decay was gone and several points were obtained which enabled the 110 minute half-life decay pattern to be established.

2.5 Data Analysis

The first step in the analysis of the data was to account for and subtract off the amount of background that was included in the total number of counts in region B.

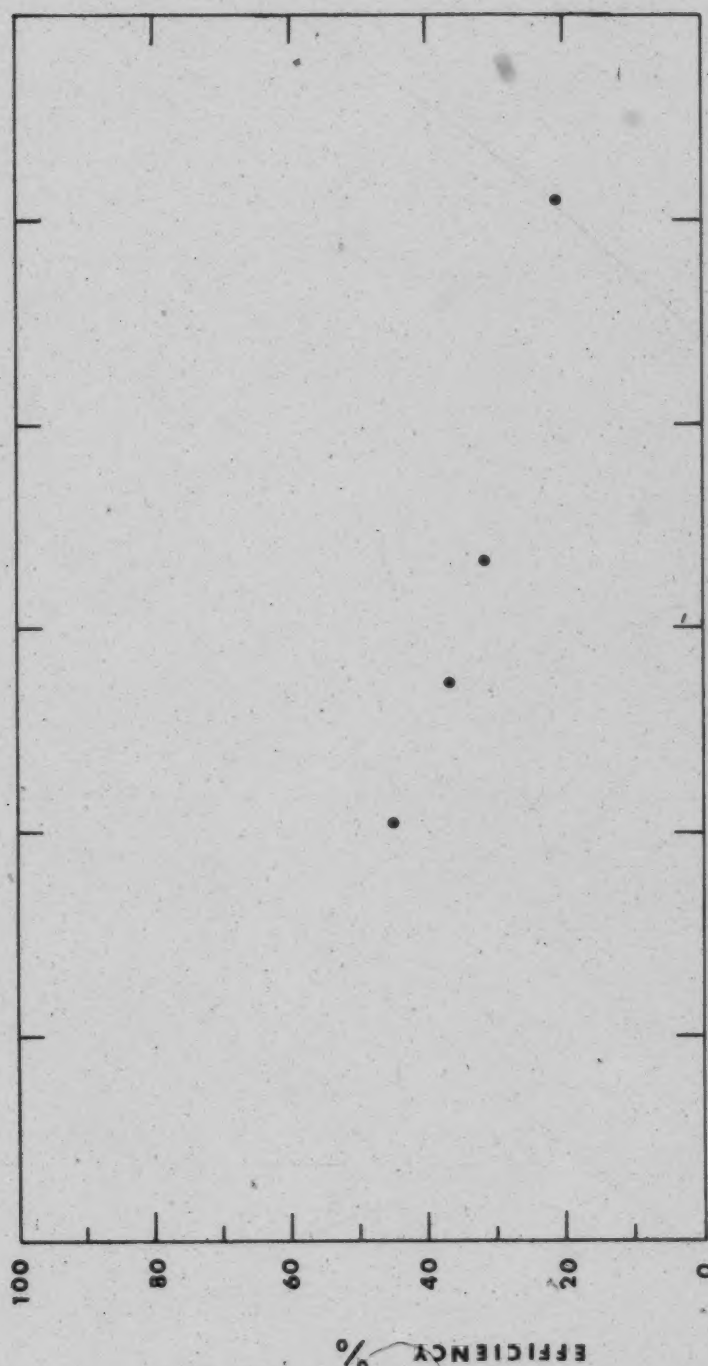

FIGURE 4 EFFICIENCY OF NaI VERSUS GAMMA RAY ENERGY

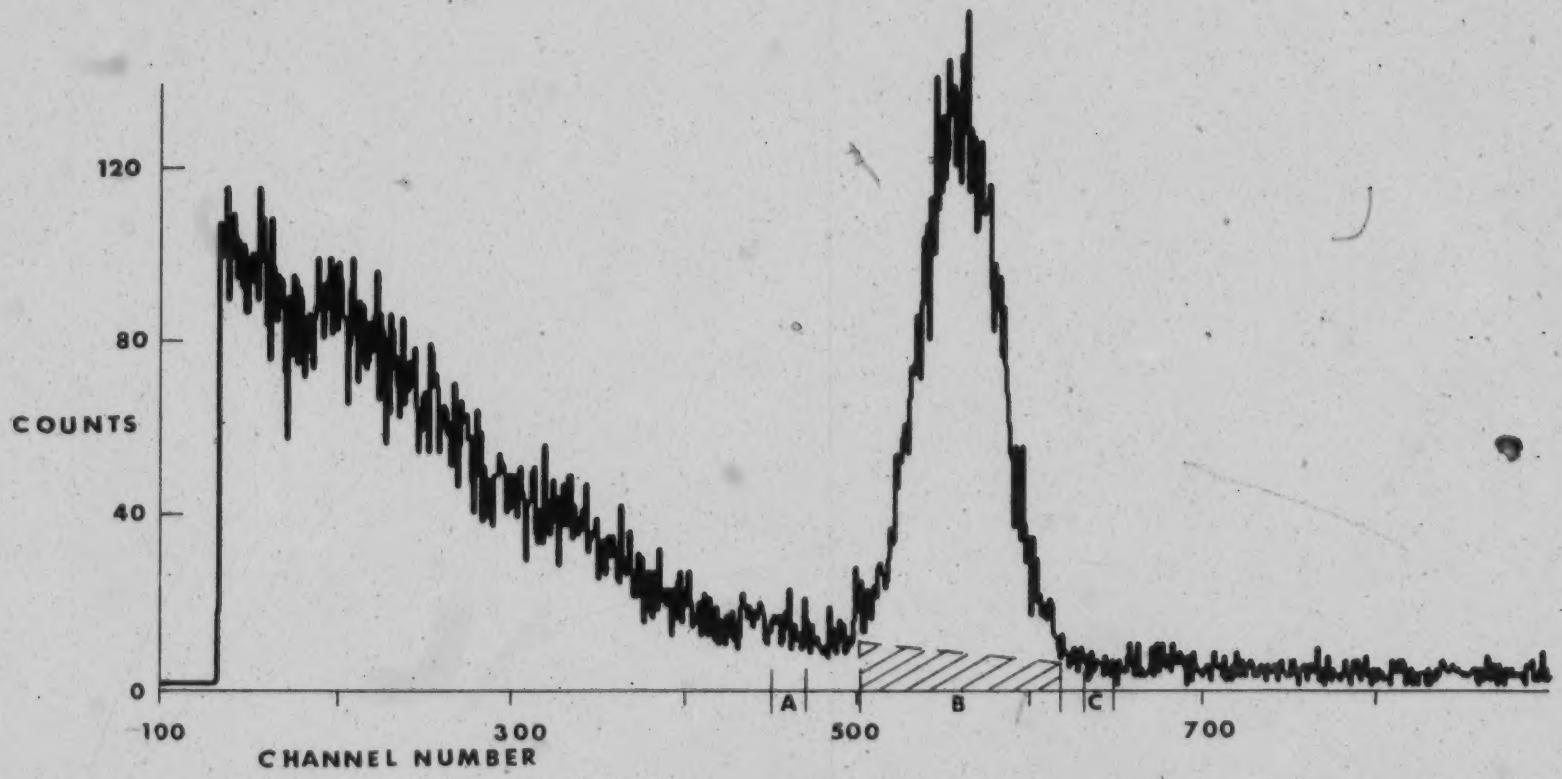

FIGURE 5 SPECTRUM FROM NaI SHOWING 0.511 MeV PEAK

A short computer program written for the PDP-8E computer did this. The program first found the average number of counts per channel in both regions A and C. Assuming that the background was linear between these two regions, the program then calculated the area of the trapezoid (cross-hatched in Figure 5) bounded by the linear background function, the zero counts line and the two boundaries of region B. This number was then subtracted from the total number of counts in B to get the number of true annihilation γ-rays counted in that minute.

This program also adjusted the number of counts in order to account for dead time in the ADC and the computer. An investigation of the change in the dead time of the system with count rate was performed using γ-ray sources, and the results are shown in Figure 6.

At this point, the data was plotted in the form of a decay curve, a typical example of which is shown in Figure 7. The time for a particular value of the count rate obtained by the above procedure was chosen to be the 30 second mark of each counting period. Time T = 0 is the instant that the beam was interrupted and the activation halted.

The data was next fed into a least squares fitting program, LSQ, which was available for use on the SDS-920 as a general purpose fitting program. The input to this program consisted of one card for each point on the decay curve for that run, each card carrying the x-component (time) and y-component (count rate) of that point, together with

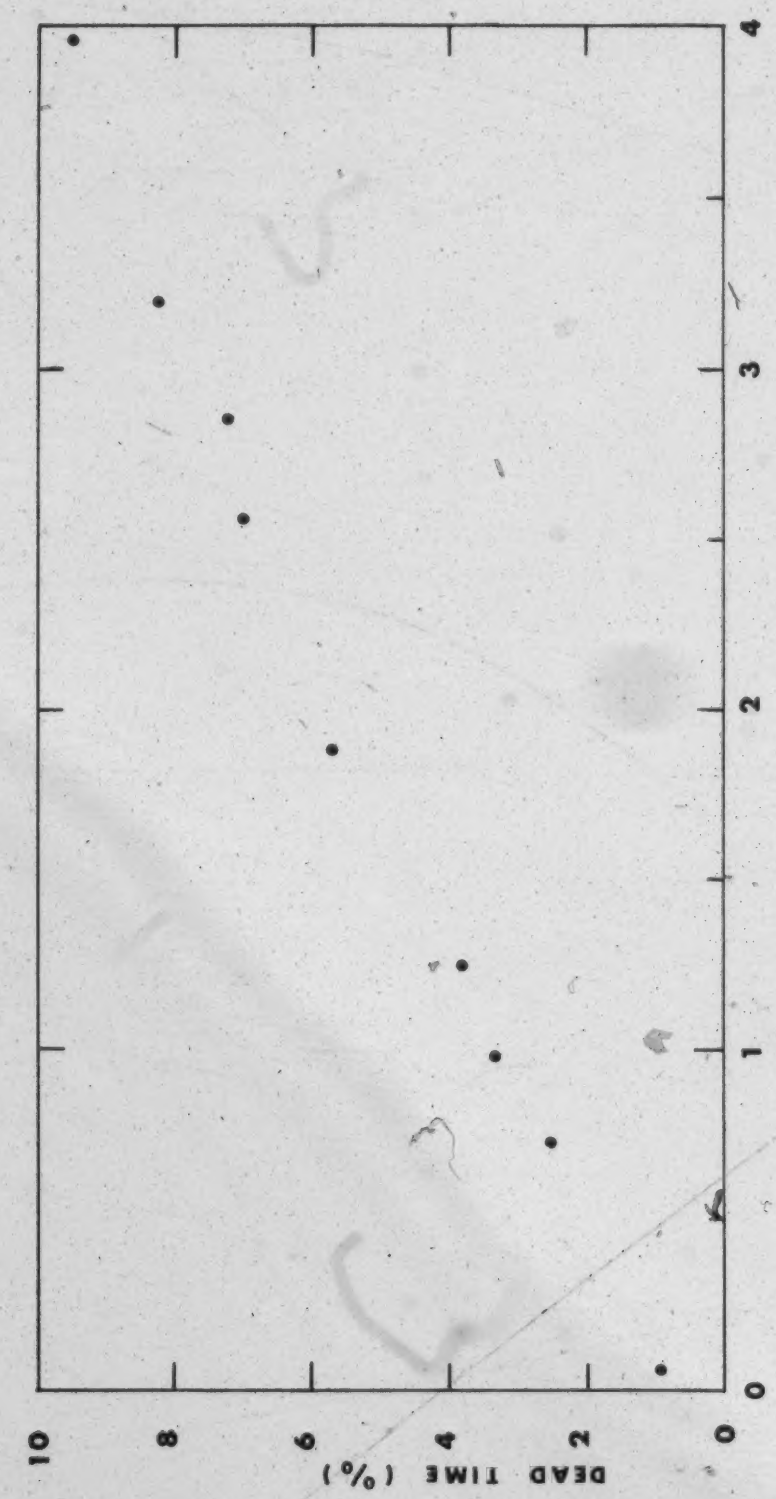

FIGURE 6 DEAD TIME OF SYSTEM VERSUS COUNT RATE

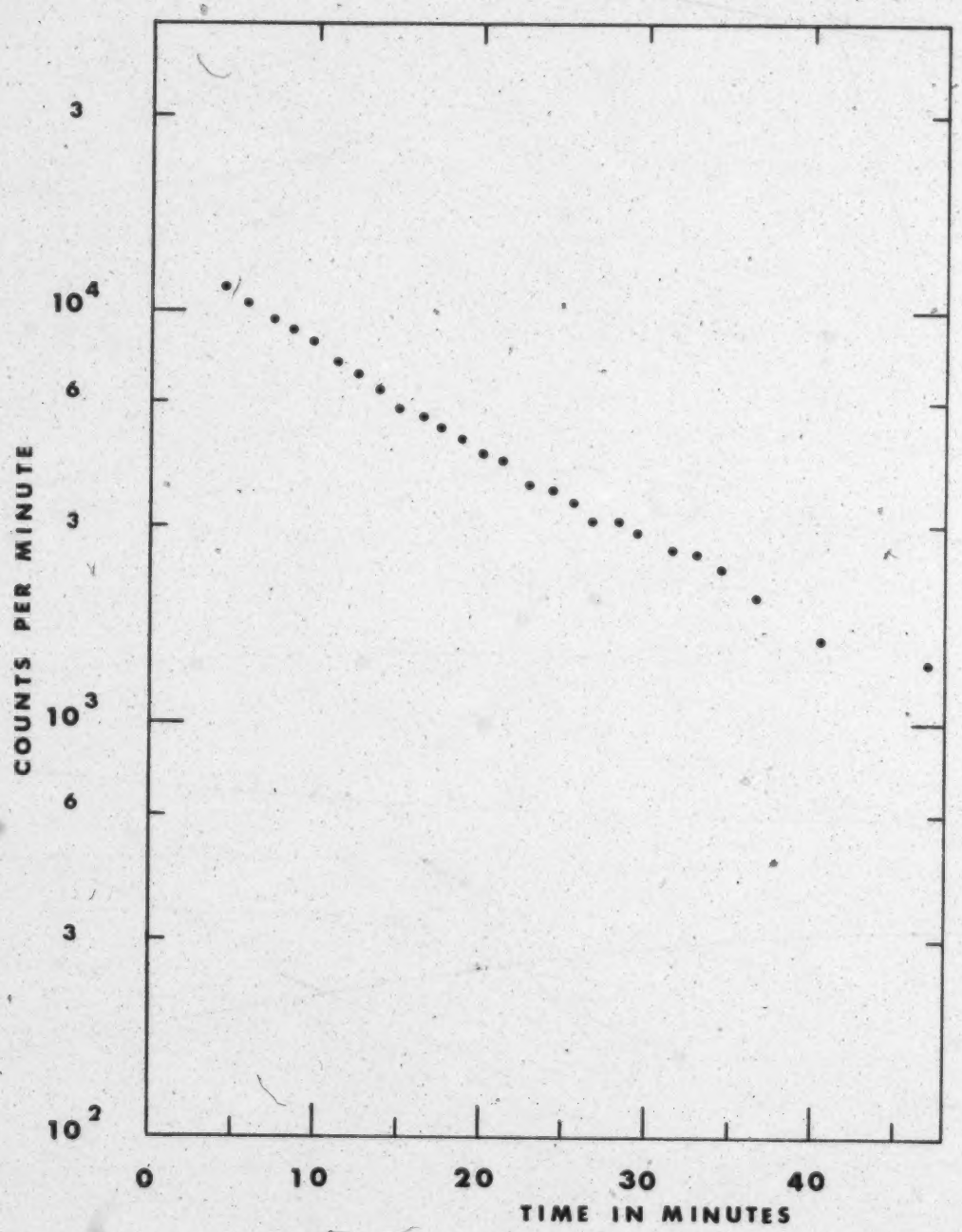

FIGURE 7 DECAY CURVE FOR ACTIVATED OXYGEN TARGET

the theoretical function which the program fitted to the experimental data. For the present experiment, the function was of the form:

$$F(t) = P_1 \exp\left(\frac{-0.693t}{P_4}\right) + P_2 \exp\left(\frac{-0.693t}{P_5}\right) + P_3 \exp\left(\frac{-0.693t}{P_6}\right) + P_7 \qquad (2\text{-}1)$$

i.e., a sum of three exponential decays of differing half-lives plus a constant. Any of the seven P_i's could be varied or held constant individually. For the present experiment, P_4 was fixed at 10.0 minutes ($\tau_{1/2}$ for ^{13}N), P_5 was fixed at 20.5 minutes ($\tau_{1/2}$ for ^{11}C, obtained by ^{14}N (p,α) ^{11}C) and P_6 was fixed at 110.0 minutes ($\tau_{1/2}$ for ^{18}F) while P_1, P_2 and P_3 were allowed to vary during the fitting. In most of the fits, the program "did not want" a constant background under the decay curve, so P_7 was fixed at zero. Because the program was fitting only linear parameters, one iteration was sufficient to achieve a minimum chi-squared for the fit. The program then printed out the parameters established and the data points (both experimental and computed).

During the analysis of various preliminary runs, all 7 parameters were allowed to vary, in order to see if there might be another half-life component in the decay. While the program had difficulty distinguishing between the 10 minute and the 20.5 minute components, in general it verified the selection of the 10.0, 20.5 and 110.0 minute half-lives.

P_1, the number of γ-rays detected that came from ^{13}N was then multiplied by an efficiency factor and a solid angle factor and divided by 2 (because there are 2 - 0.511 MeV γ-rays emitted per β^+ annihilation) to obtain the number of β^+ particles emitted per minute from the ^{13}N nuclei in the target at time T = 0 (this number was denoted by the symbol A_o).

The cross sections were then calculated using the formula given in Appendix B.

2.6 Results and Discussion

The cross section for ^{16}O (p,α) ^{13}N was measured at eleven points between 6.5 and 7.7 MeV. Below 6.5 MeV the cross section was too low to be detected by the present experimental configuration.

Before discussing the main results, however, the details of two consistency checks will be given. In order to check the validity of the experimental procedure and the calculations used in the analysis of the data, the cross section of the reaction ^{13}C (p,n) ^{13}N was measured at 5.80 MeV, using precisely the same procedure as was used for the ^{16}O (p,α) reaction. The target used was a 150 $\mu gm/cm^2$ carbon target, enriched to 95 per cent in ^{13}C, to which an aluminum catcher foil was attached. The cross section for this reaction has been determined previously to be 150 mb (Dagley et al., 1961). The cross section measured using the present method was 142 ± 12 mb, in excellent agreement with the

first value.

The second consistency check was to measure the ^{16}O (p,α) ^{13}N cross section below threshold, where, of course, it must be zero. The result obtained was 16μb, which is consistent with zero within the uncertainties of the experiment. This result also effectively determined the lower limit on the cross section that could be measured, due to statistical uncertainties and errors introduced in subtracting contributions due to the ^{13}C (p,n) ^{13}N reaction.

This procedure was repeated for each of the MgO_2 targets used in the experiment (4 or 5) in order to determine the nitrogen content of the targets, if any, using the magnitude of the ^{14}N (p,α) ^{11}C reaction cross section, which is well known over the range of energies used in this experiment (Bodansky et al., 1972). The nitrogen content of one target was found, in this manner, to be 0.002 times the oxygen content of that target. Unfortunately, the ^{14}N (p,p) differential cross sections are not known in this region, but it is reasonable to expect that the cross section is the same order of magnitude as the oxygen cross section. Thus, for a run long enough to accumulate 100,000 counts in the oxygen elastic scattering peak, the nitrogen peak would contain 200 counts, which could not be seen above background. Even if the ^{14}N (p,p) cross section was an order of magnitude higher than estimated above, the peak would not be significant above background.

The ^{16}O (p,α) ^{13}N cross sections are presented in

Table 1, as well as Figure 8. As can be seen, the cross section, once detectable, rises extremely rapidly, increasing by a factor of 200 within 1 MeV.

The penetration factor for an alpha particle leaving the compound nucleus, ^{17}F, which is discussed in Appendix A, has been applied to the low energy cross sections. The factor is calculated as a function of energy and then normalized to some particular cross section so that the curve describes the shape of the cross section as well as possible. As can be seen in Figure 8, and as expected, the penetration factor follows the shape of the data very well. The advantage of having this functional form for the cross section at low energy is that it can be used to estimate the cross section at some point, e.g., 6.3 MeV, where it cannot be easily measured experimentally.

The main errors in these cross sections, given in Table 1, come from three sources: the uncertainty in the efficiency determination of the scintillation counter, the uncertainty in the elastic scattering cross sections, and the uncertainty in the determination of A_o. The errors in the efficiency calculation stem from the uncertainties in the calibrated γ-ray source strengths, which were stated by the manufacturers* as ± 4 - 5 per cent. The elastic

---

*New England Nuclear Corporation, Boston, Mass.

TABLE 1

CROSS SECTION vs. ENERGY

FOR ^{16}O (p,α) ^{13}N

E_p^{LAB} (MeV)	$\sigma(E)$ (mb)	ERROR (mb)*
6.51	0.050	0.020
6.64	0.050	0.019
6.71	0.250	0.043
6.78	0.330	0.045
6.91	1.16	0.09
7.01	2.63	0.14
7.11	2.82	0.16
7.21	4.92	0.24
7.31	11.60	0.58
7.51	11.55	0.68
7.71	13.80	0.83

* This column lists the root-mean square of the uncertainties given in the text.

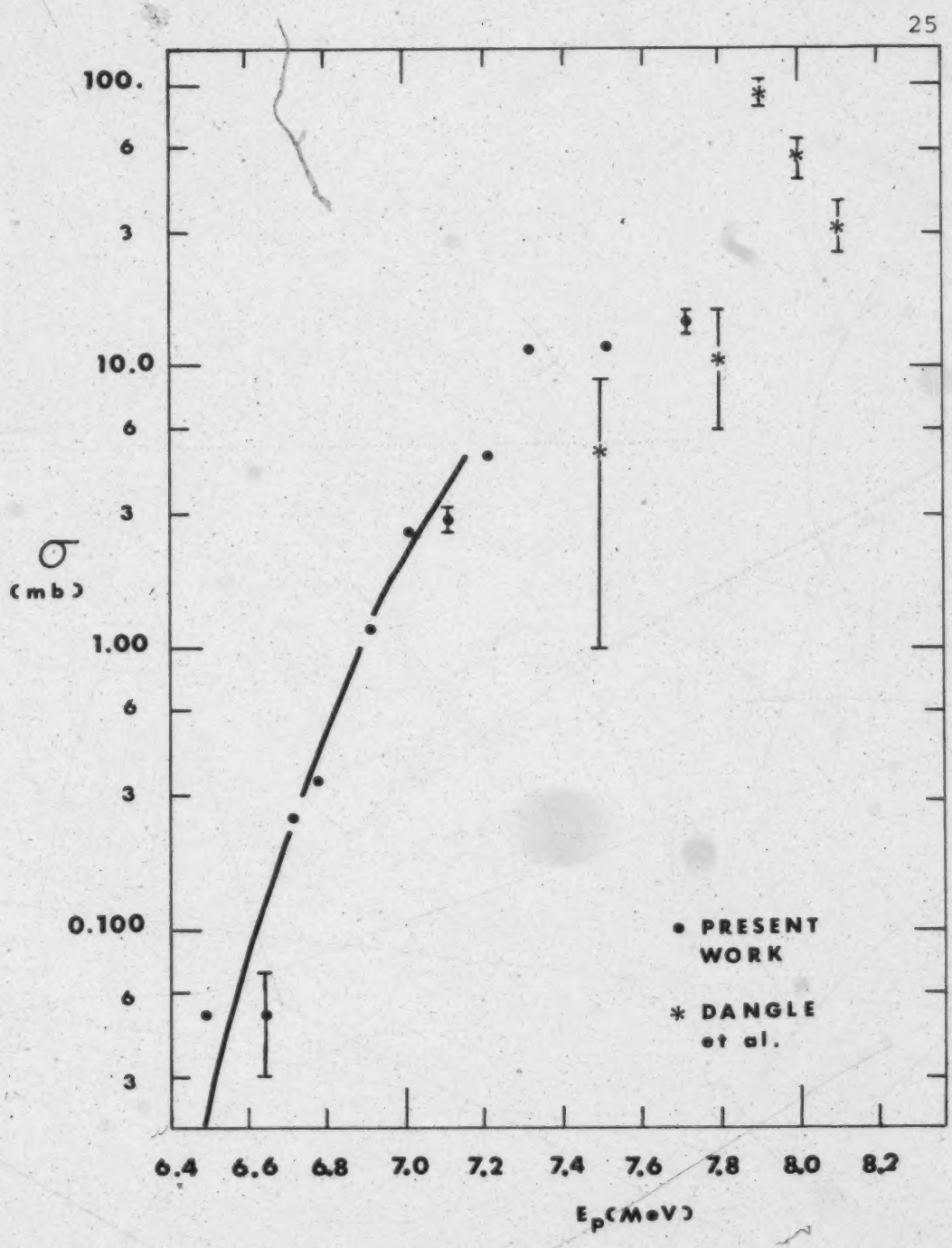

FIGURE 8 TOTAL CROSS SECTION OF $^{16}O(p,\alpha)^{13}N$ WITH PENETRATION FUNCTION

scattering cross sections were stated in the original paper (Salisbury et al., 1962) as ± 0.5 per cent. However, the absolute error in reading the figures from a small graph was estimated as ± 5 mb/sr, with the relative error varying between 2 per cent and 10 per cent, depending upon the cross section at that energy and angle. The uncertainty in A_o resulted from statistical uncertainties and from uncertainties in the fitting procedure, and was obtained from an error matrix which was printed by the program LSQ. This matrix gave the variance in each of the variable parameters, and the variance for the 10 minute half-life parameter, P_1, was changed into a percentage by taking its square root, and dividing by P_1. This error varied from 20 per cent at the low energy end of the experiment to < 1 per cent at the higher energies. In addition, a systematic error of 16μb resulting from the uncertainty in determining zero cross section was inserted, but was significant only for the four lowest cross sections.

As is discussed in Appendix A, the range of energies over which the cross section is important extends somewhat higher than this experiment covered. Therefore, it was necessary to integrate the differential cross sections of Dangle (Dangle et al., 1964) for this reaction at some higher energies. The integration was done numerically using an even-order Legendre polynomial fitting program. The integrated cross sections at 7.50 MeV (5.0 ± 4.0) mb and 7.80 MeV (11.3 ± 5.0 mb) were compared with the present

data, and are seen in Figure 8 to be in general agreement. The cross sections at the higher energies were used in the calculation of the reaction rate. The large errors in these figures come mainly from the integration procedure and reading the differential cross sections from a small graph.

The reaction rate $\lambda = \langle \sigma v \rangle$ was calculated according to the formula given in Appendix A. The integration was done numerically by an application of Simpson's rule, and covered the range from 6.50 MeV laboratory proton energy to 8.10 MeV. The temperature used for the integration was 3.5×10^9 °K. The reaction rate was found to be $N_A \lambda = 0.049$ cm^3/gm-sec. This is to be compared to Wagoner's estimate (Wagoner, 1969) for this reaction of $N_A \lambda = 0.308$ cm^3/gm-sec, which is substantially larger than the present measurement.

It should be noted that in neither our final cross sections nor in several preliminary runs that were made were any indications of sharp resonance behavior evident.

CHAPTER III

THE ^{10}B (α,n) ^{13}N REACTION

3.1 Accelerators

Because, as is discussed in Appendix A, the important energy range for this reaction is below 1.2 MeV, it was decided to perform this experiment on the 2.0 MeV Van de Graaff Accelerator of the University of Alberta Chemistry Radiation Laboratory. Some runs were also taken using the 7.5 MeV Van de Graaff Accelerator, which was used for the first experiment.

3.2 Targets

The targets used in this experiment were made from elemental boron, enriched to 94.89 per cent in ^{10}B, supplied by the Oak Ridge National Laboratory, Oak Ridge, Tennessee. Because boron has such a high melting point (2300°C), it was necessary to evaporate it using an electron-gun. The 170 $\mu gm/cm^2$ aluminum foil was again used as a target support and catcher foil. The targets had a thickness of approximately 30 $\mu gm/cm^2$. During some preliminary runs, a natural boron target of about 5 mm thickness was used in order to take advantage of the fact that because of its thickness, the target integrated the cross section over a wide range of energies. This target was made by compressing

powdered boron into a pellet using a hydraulic press.

3.3 Target Thickness Determination

The thickness of the targets was measured using the technique employed during the previous experiment. The only modification to the beam line (Figure 1) was to add a guard ring, maintained at a potential of -100 volts directly in front of the Faraday cup in order to suppress secondary electrons from the Faraday cup. Protons of 5.30 and 5.50 Mev were used, and the scattered protons were detected at 165°. The energies and angle used were chosen because the ^{10}B (p,p) differential cross section (Watson et al., 1969) was appreciable (around 100 mb/sr) and was a slowly varying function of angle.

Examination of the spectra showed that there were very few contaminants present in the target to any great extent. However, this was not a major problem during the present experiment, as there were no reactions possible with any common contaminants (e.g., carbon or oxygen) that led to β^+ unstable nuclei.

3.4 Activation Procedure

The beam line configuration used for the experiments done at the Chemistry Radiation Laboratory is shown in Figure 9. The alignment of the beam line was checked at various stages of construction using a laser beam that was aligned along the required line of travel of the alpha particles. The magnet image slits had a diameter of 5/32".

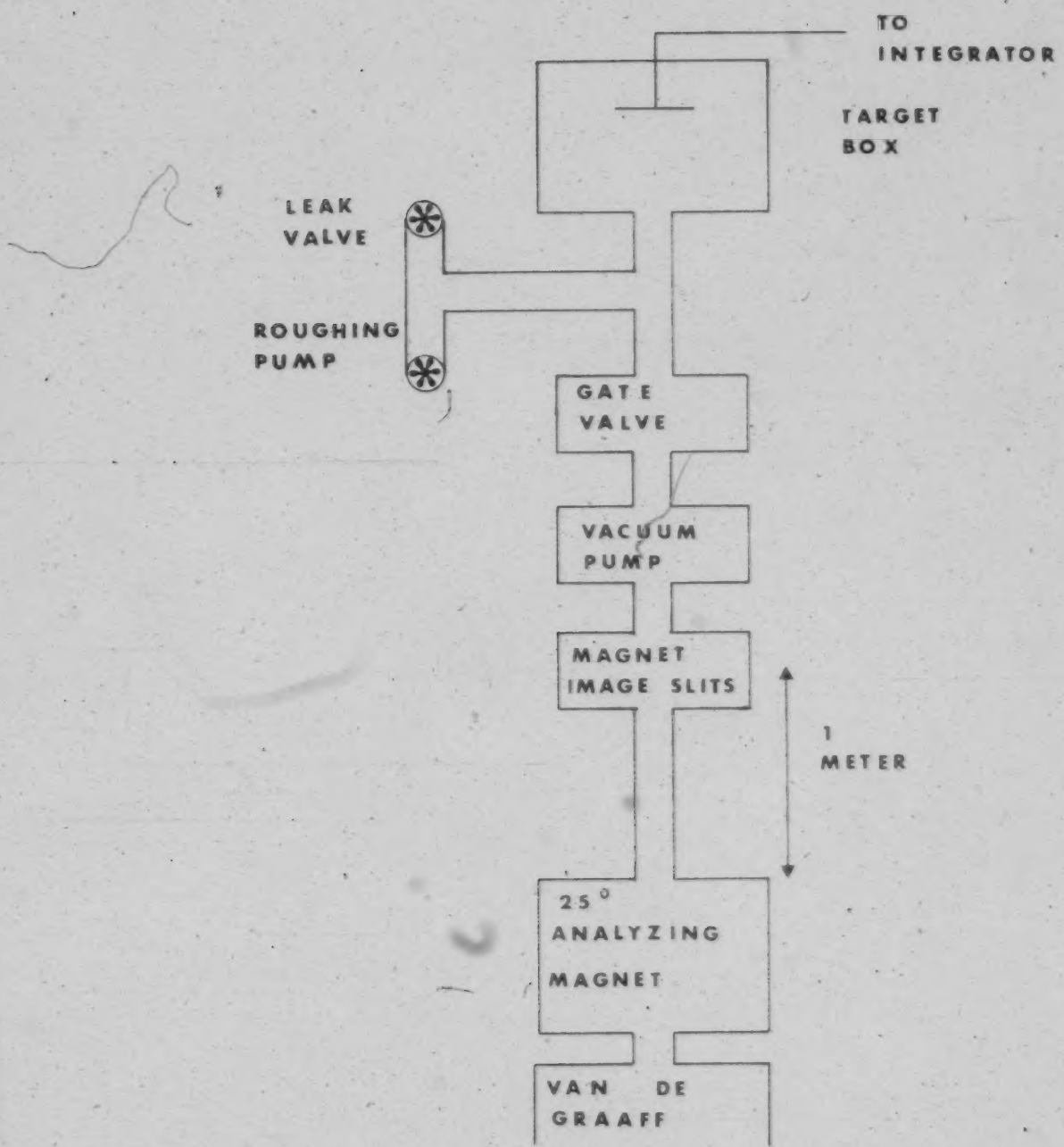

FIGURE 9 SCHEMATIC BEAM LINE CONFIGURATION AT THE CHEMISTRY RADIATION LABORATORY

The target chamber was a 4" diameter slit box which was modified in order to hold a sliding seal mechanism which enabled the target to be rotated or moved vertically without breaking vacuum. Just at the entrance to this chamber, a 13/32" collimator was placed in order to properly define the beam. Also, an 11/16" inside-diameter ring on a teflon stand was placed approximately one inch in front of the target and was biased at -300 volts in order to provide electron suppression. A detailed sketch of the target chamber is shown in Figure 10. A piece of tantalum thick enough to completely stop the beam was placed directly behind the target and the target was placed at a potential of +45 volts to provide additional suppression. The charge incident upon the target was collected and integrated.

A basic assumption in the calculation of the cross section (Appendix B) is that the incoming beam was constant over the activation period. The beam obtained from the 2.0 MeV Van de Graaff was, however, very unstable, so in order to compensate for this, the "beam-averaging" RC circuit in Figure 11 was used to "integrate" the charge collected at the target. Switch S_1 (normally closed) was provided so that when opened, all the current went through the resistance R, providing a voltage reading V_{max} which, knowing R, gave an instantaneous value for the beam current. The value of the resistance was determined to be R = 72 megohms ± 2 per cent, and C was chosen so that the time constant of the circuit was equal to 10 minutes (the half-life of ^{13}N)

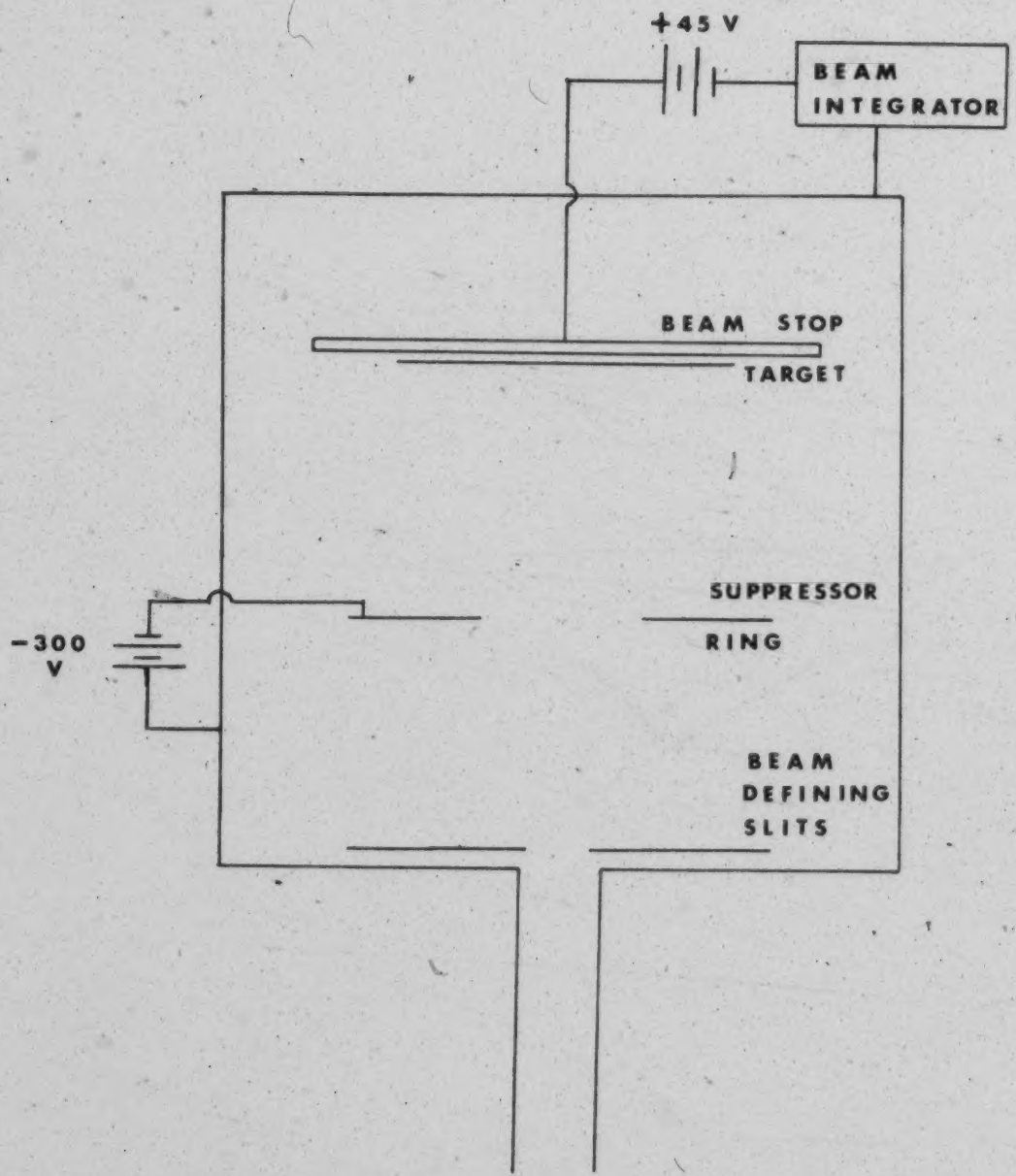

FIGURE 10 ENLARGED VIEW OF TARGET BOX

FIGURE 11 BEAM AVERAGING RC CIRCUIT

($C \simeq 8.5$ μf).

With a steady beam, the voltage across the capacitor at any time divided by the maximum voltage V_{max} was in the same ratio as the fraction of equilibrium activation that the target had achieved. Then, when the beam was lost, the voltage across the capacitor decayed at the same rate that the target decayed. Thus, with an unsteady beam current, this circuit mirrored the production and decay of the product nucleus with time.

In these runs, when the voltage reached 0.865 times V_{max}, the target had undergone an activation equivalent to a bombardment for 2 half-lives with a steady beam current I (given by $I = V_{max}/R$). At this point, the run was terminated and the target was removed to the counting apparatus.

Although the beam from the 7.5 MeV machine was not unsteady enough to require the use of this device, it was used in order to keep the experimental procedure invariant. Also the same target chamber, collimators and biases were used for both experiments, except that the beam-defining slits at the entrance to the target box were reduced from 13/32" to 9/32".

3.5 Counting Arrangement

After the target was activated, it was placed between two 3" x 3" NaI (Tl) scintillation counters, which were used in coincidence to count the 0.511 MeV annihilation

γ-rays. The counters were held in the plexiglass stand shown in Figure 12. This stand held the counters firmly so that both detectors were the same distance from the source (or target) between them and the axes of both counters were colinear. The stand was constructed so that the front face of each detector could be placed 1, 3, or 5 inches from the target. The base of the stand had a slight indentation in it so that the target ladder used could be placed in the same position every time. An aluminum sleeve was placed over the target to ensure the annihilation of the β^+ particles. For the Chemistry Radiation Laboratory, a 2" lead brick cave was constructed around each scintillator, with a small opening to insert the target, in order to reduce background. This cave was not necessary for the experiments done at the Nuclear Research Centre.

The signals from the two NaI counters were sent into the electronics arrangement shown schematically in Figure 13. After being amplified, the signals were fed into a single channel analyser (SCA) which was used to set a window on the 0.511 MeV γ-ray peak in each spectrum. The SCA output signals were then sent to a coincidence unit. A dual counter-timer was used to count the coincidence signals for a preset time. When the time was reached, the printout control would automatically print out the number of counts registered and the time on a teletype unit, reset the counter-timer, and restart it. The time taken to print out the values and restart the counting was about 2.6 seconds.

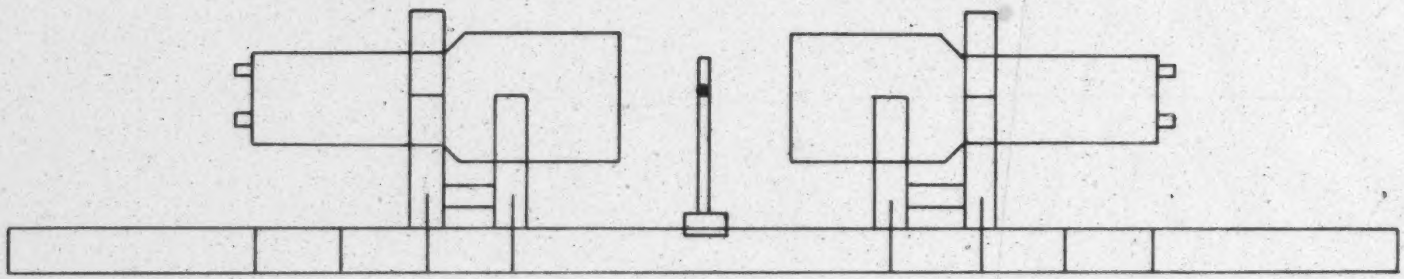

FIGURE 12 COINCIDENCE NaI COUNTING STAND
(NOT TO SCALE)

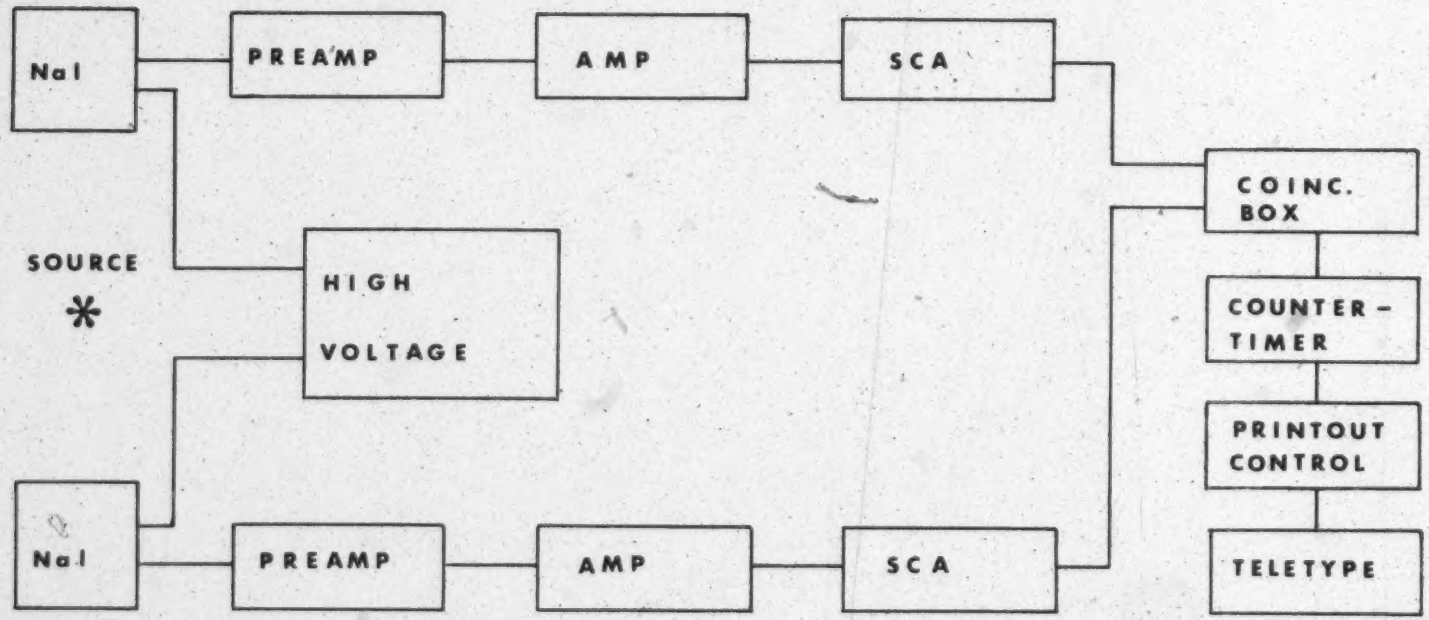

FIGURE 13 SCHEMATIC - COINCIDENCE ELECTRONICS DIAGRAM

Using the above arrangement, the number of background coincidences was found to be less than 5 per minute. The efficiency of the scintillation counters was determined by counting the number of coincidences registered from a ^{22}Na source of known activity. The absolute efficiency of the arrangement with the NaI detectors both 1" from the source was approximately 5 per cent.

The decay rate of the activated nuclei was monitored for about 50 to 60 minutes after each bombardment stopped.

3.6 Data Analysis

The data obtained via the teletype was first plotted to give a decay curve, a typical example of which is shown in Figure 14. As can be seen by comparing this curve with Figure 7, the decay curve obtained during the oxygen experiment, the present results indicate a pure 10-minute half-life decay, as opposed to the many-component character of Figure 7.

The data was then used as input to the program LSQ, discussed in Section 2.5. The theoretical function was of the same form as eq. 2-1 except that P_2 and P_3 were fixed at zero, thus reducing the function to that of a single decay component plus a constant background. The amount of background assigned by the program was in every case negligible compared to the amount of 10-minute activity. The fits obtained by the program were excellent in almost every instance, the only exceptions being those runs at

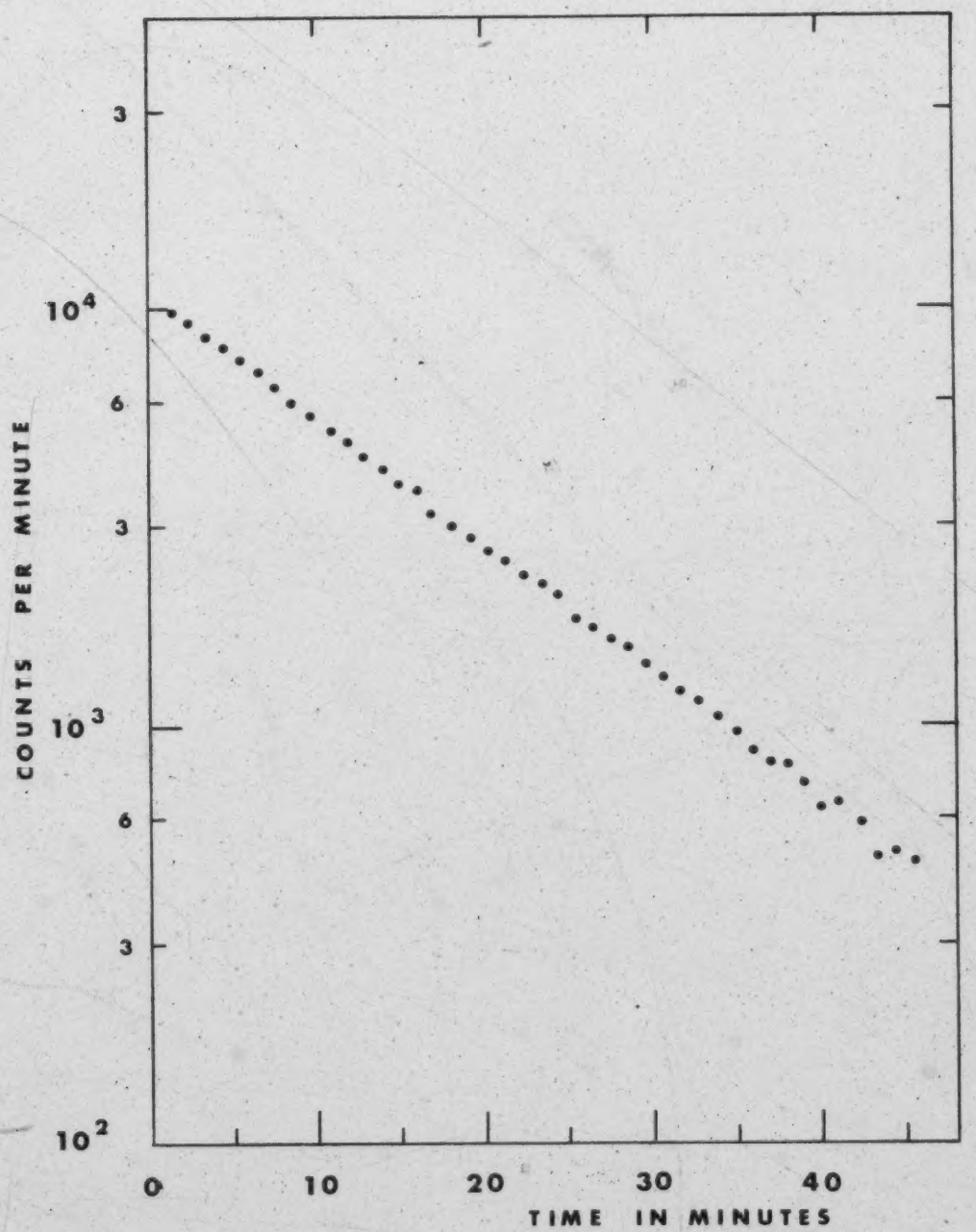

FIGURE 14 DECAY CURVE FOR ACTIVATED BORON TARGET

energies with very low cross sections, where the counting statistics were very poor.

The number P_1, output by the program was multiplied by an efficiency factor to yield the quantity A_o, and the cross sections for the ^{10}B (α,n) ^{13}N reaction were found using the formula given in Appendix B.

3.7 Results and Discussion

The ^{10}B (α,n) ^{13}N cross section has been measured in this experiment at 24 points below 1.61 MeV, although some of these points are at almost the same energy. The first cross section large enough to be detectable by the present method is at 1.15 MeV, although several runs were taken at energies down to 0.75 MeV to verify that the cross section remained below the detectable limit to that point. At 1.1 MeV, the 5 mm thick target described above was used and no activation was observed. Because this target was thicker than the range of 1.1 MeV alphas, the cross section integrated from 0 to 1.1 MeV would be measured. The fact that no activation was observed indicated that the cross section does not have any resonances in it below 0.75 MeV large enough to be detectable in this experiment.

The cross sections determined in this experiment are listed in Table 2 and are shown in Figure 15. Those cross sections listed above the line in Table 2 and shown by dots in Figure 15 were found from runs at the Chemistry Radiation Laboratory (CRL) while those listed below the

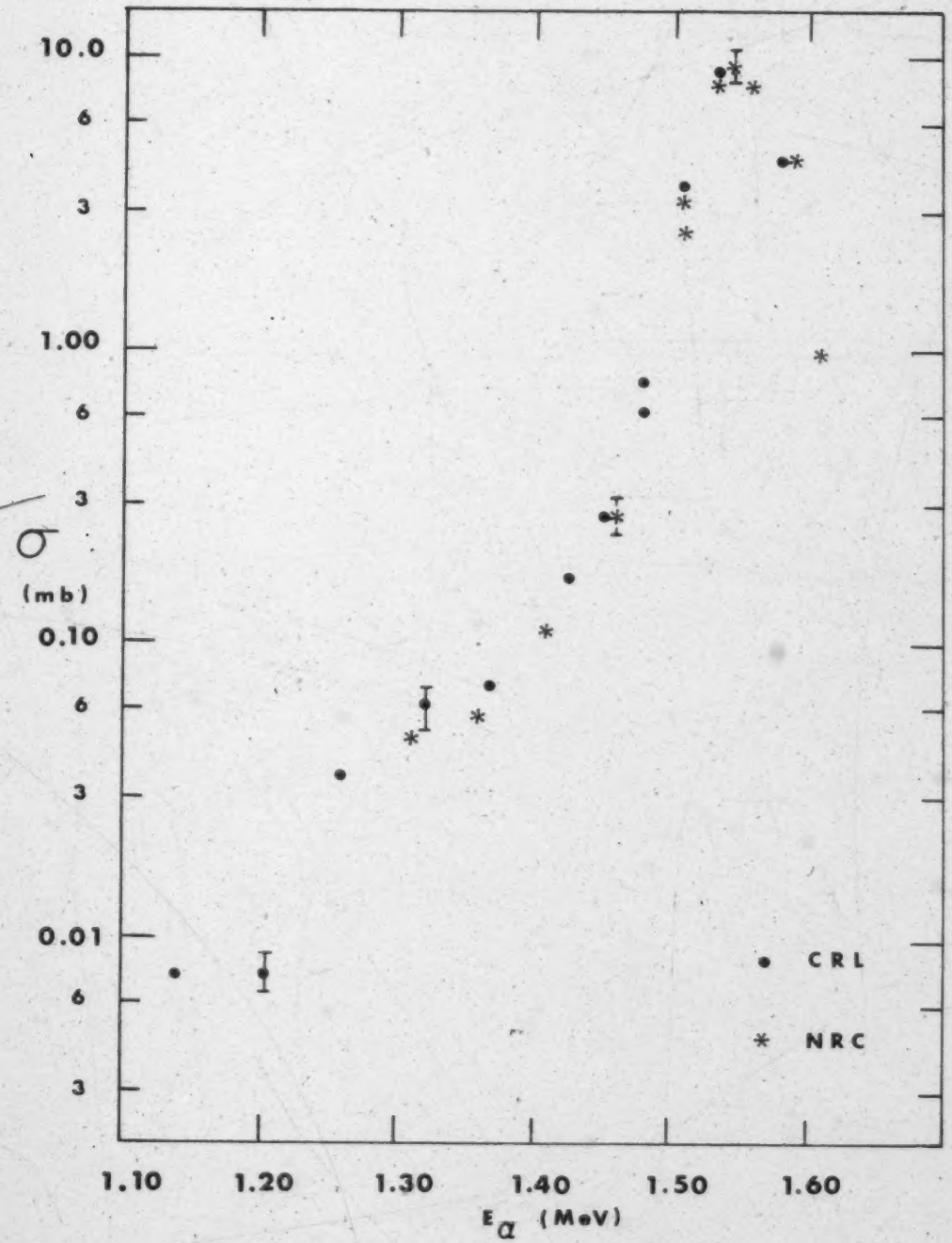

FIGURE 15 TOTAL CROSS SECTION OF $^{10}B(\alpha,n)^{13}N$ VERSUS ENERGY

TABLE 2

^{10}B (α,n) ^{13}N CROSS SECTION vs. ENERGY

E_α (MeV)	σ (mb)
1.579	4.38
1.535	8.68
1.535	8.67
1.508	3.62
1.483	.78
1.481	.62
1.453	.27
1.425	.17
1.370	.072
1.319	.061
1.264	.035
1.206	.0075
1.151	.0077
1.610	0.97
1.585	4.40
1.560	7.79
1.545	9.28
1.535	8.30
1.510	3.36
1.510	2.65
1.460	.27
1.410	.11
1.360	.058
1.310	.048

line and shown by crosses were found at the Nuclear Research Centre (NRC).

Due to some questions as to the accuracy of the energy calibration of the 2.0 MeV machine, the experiment was repeated using the 7.5 MeV machine. An energy difference was found and corrections were made.

The two cross sections at 1.535 MeV at the CRL were done with the same target at the beginning and end of the experimental period to verify that the results were reproducible and that the target was not flaking away with time. The closeness of the results, 8.67 and 8.68 mb, confirms both points.

In an examination of Figure 15, the agreement between the two sets of data is excellent. Runs taken at the same energies at different accelerators agree extremely well, and the resonance in the cross section is determined very well.

The resonance peaks at 1.545 MeV whereas previous work by Shire (Shire et al., 1953) had placed the resonance at 1.51 MeV. The relevant energy level in ^{14}N is a 3^- state at 12.69 MeV (Ajzenberg-Selove, 1970) and corresponds to $E_\alpha = 1.51$ MeV. The energy discrepancy in the present work could be the result of a small error in the calibration of the NRC machine.

There is also in the data a strong indication that a "shoulder" exists on the cross section at about 1.33 MeV, which would suggest that a very wide, weaker resonance

occurs near this point. This would indicate that the 3^+ state of ^{14}N at 12.61 MeV (Ajzenberg-Selove, 1970) (E_α= 1.40 MeV) can neutron decay, which has not been previously reported.

In the present experiment, the peak cross section is 9.3 mb. This is in sharp contrast to the results of Shire et al., who find that the cross section peaks at 32mb. Some of this difference could be due to averaging of the cross section over the thickness of the targets (which were $\approx$ 10 keV thick). However, Shire et al., state that due to difficulties in estimating the target thickness and the gradual deterioration of their targets, their results could be in error by a factor of 2. Their neutron detection apparatus could also add errors to their figures, bringing them more into agreement with the present results.

The error bars for four typical points are shown in Figure 15. The errors range from over 16 per cent at the low cross section points to about 12 per cent near the peak of the cross section. An error of 5 per cent was introduced in all runs from the uncertainty in the calibrated γ-ray sources, as in the ^{16}O (p,α) experiment. The error incurred in getting the elastic scattering cross section and thus the target thickness is estimated to be 10 per cent. The errors in the determination of A_o range from 0.2 per cent at the peak to > 10 per cent at points of low cross section. In addition, a 5 per cent error was assigned due to the method of averaging out the beam current, caused mainly by the

error in setting the time constant for the RC circuit at 10.0 minutes. The root-mean-square of the individual errors is 12 to 16 per cent, as mentioned above.

Assuming a value for the temperature of $T = 2.5 \times 10^9$ °K, the cross section was numerically integrated as described in Chapter II and Appendix A to give the reaction rate. Using the experimental cross sections, the reaction rate was found to be $N_A \lambda = 1.9 \times 10^4$ cm^3/g-sec. The rate given by Wagoner (Wagoner, 1969) for the same temperature is 57.2×10^4 cm^3/g-sec, which, as for the ^{16}O (p,α) reaction, is considerably higher than the experimental reaction rate.

CHAPTER IV

CONCLUSIONS

The activation procedure used for the present experiments is a simple and reliable method of determining cross sections of reactions leading to nuclei with suitable half-lives. With minor modifications to the present procedure, the decay pattern of nuclei with half-lives from several seconds to a couple of days could easily be established. The chief advantage of this method is that it eliminates the long process of taking angular distributions and the necessity (and the errors) of integrating that distribution. Also, reactions are astrophysically important, generally, only at very low energies where the exiting particles are even harder to detect.

The reaction rate for the ^{16}O (p,α) ^{13}N reaction has been found to be 0.049 cm^3/g-sec, as compared with the previous estimate of 0.308 cm^3/g-sec. The rate for the ^{10}B (α,n) ^{13}N reaction was determined to be 1.9×10^4 cm^3/g-sec, as compared to the estimate of 57.2×10^4 cm^3/g-sec. These reductions will cause significant changes to various models of stellar evolution. They also indicate that the estimates for reaction rates made by Wagoner should be used with care until more experimental tests of the estimates have been done.

In conclusion, then, the present work has shown the need for more experimental determinations of rates of nuclear reactions important to calculations of stellar evolution and nucleosynthesis.

REFERENCES

REFERENCES

Ajzenberg-Selove, F.
1970 Nucl. Phys. A152, 1.

Arnett, W. D., and J. W. Truran.
1969 Ap. J. 157, 339.

Bodansky, D., D. D. Clayton, and W. A. Fowler.
1968 Ap. J. Suppl. 148, 16, 299.

_____, W. W. Jacobs, D. Oberg, and P. Russo.
1972 Nuclear Physics Laboratory Annual Report, University of Washington, p. 67.

Clayton, D. D.
1968 Principles of Stellar Evolution and Nucleosyntheses. McGraw-Hill, New York.

Cohen, B. L.
1955 Phys. Rev. 100, 206.

Dagley, P., W. Haeberli, and J. X. Saladin.
1961 Nucl. Phys. 24, 353.

Dangle, R. L., L. D. Opplinger, and G. Hardie.
1964 Phys. Rev. 133, B647.

Salisbury, S. R., G. Hardie, L. D. Opplinger, and R. Dangle.
1962 Phys. Rev. 126, 2143.

Sharma, T. C.
1973 Ph.D. Thesis, University of Alberta, Unpublished.

Shire, E. S., J. R. Wormald, G. Lindsay-Jones, A. Lunden,
1953 and A. G. Stanley.
Phil. Mag. 44, 1197.

Swint, J. B., A. C. L. Barnard, T. B. Clegg, and J. L. Weil.
1966 Nucl. Phys. 86, 119.

Wagoner, R. B.
1969 Ap. J. Suppl. 162, 18, 247.

Watson, B. A., P. P. Singh, and R. E. Segel.
1969 Phys. Rev. 182, 977.

Woosley, S. E.
1973 Submitted for publication to Ap. J.

Woosley, S. E., W. D. Arnett, and D. D. Clayton.
1972 Phys. Lett. 38B, 196.

Woosley, S. E., W. D. Arnett, and D. D. Clayton.
1973 Submitted for publication to Ap. J. Suppl.

APPENDICES

APPENDIX A

RELEVANT ASTROPHYSICAL THEORY

For nuclear physicists, the cross section σ for a particular reaction with a center of mass energy E is a meaningful and useful quantity, because they deal almost exclusively with monoenergetic beams of particles incident upon a stationary target. However, for astrophysicists working with stellar interiors, $\sigma(E)$ is not useful, because they are dealing with particles which move with a broad spectrum of energies. Therefore, a quantity called the reaction rate per pair of particles is defined by (Clayton, 1968, p. 292):

$$\lambda = \langle \sigma v \rangle = \int_0^\infty \sigma(v)\ v\ \phi(v)\ dv \qquad A1$$

where v is the relative velocity between the two particles, and $\phi(v)\ dv$ is the probability that the relative velocity between the two particles has a magnitude $v \pm dv$, such that $\int_0^\infty \phi(v)\ dv = 1$. That is, the reaction rate is the cross section multiplied by the relative velocity with the product being averaged over an appropriate velocity distribution. It may also be written as:

$$\lambda = \int_0^\infty \sigma(E)\ v(E)\ \Psi(E)\ dE \qquad A2$$

Stellar interiors are very complicated and obtaining the quantity ϕ (or ψ) exactly is impossible. A very common assumption is that the stars are in local thermodynamic

equilibrium. With this assumption, it can be shown that the distribution of relative velocities is given by Maxwell-Boltzmann statistics, i.e. (Clayton, 1968, p. 300):

$$\psi(E)\,dE = \frac{2}{\sqrt{\pi}} \frac{E}{kT} \exp\left(\frac{-E}{kT}\right) \frac{dE}{(kTE)^{1/2}} \qquad A3$$

where k is Boltzmann's constant, and T is the temperature, in °K. Inserting this relation into A2 yields:

$$\lambda = \frac{2}{\sqrt{\pi}} \frac{1}{(kT)^2} \sqrt{\frac{2kT}{\mu}} \int_0^\infty \sigma(E)\, E \exp\left(\frac{-E}{kT}\right) dE \qquad A4$$

For a particular reaction and temperature, the terms in front of the integral are constant. It is also convenient to speak of $N_A \lambda$ ($N_A \equiv$ Avogadro's number) instead of λ.

At low energies, the cross section for any charged particle reaction is predominantly determined (assuming that there are no resonances) by the fact that the particles must either penetrate a Coulomb barrier to combine with each other (e.g., $^{10}B + \alpha \rightarrow {}^{13}N + n$) or must penetrate the barrier in order to escape the compound nucleus (e.g., $^{16}O + p \rightarrow {}^{13}N + \alpha$). This penetration factor has been shown to be proportional to:

$$PF \propto \exp\left(-b\, E^{-1/2}\right) \qquad A5$$

where b is a parameter given by (Clayton, 1968, p. 299):

$$b = 31.28\, Z_1\, Z_2 \sqrt{\frac{A_1 A_2}{A_1 + A_2}} \qquad [(keV)^{1/2}] \qquad A6$$

Thus the cross section of a reaction at low energies should also be proportional to this factor.

Now, returning to eq. A4, the integral is a product

of three terms:

$$I\alpha \int_0^\infty \exp\left(-bE^{-1/2}\right) E \exp\left(\frac{-E}{kT}\right) dE \qquad A7$$

The first term in this expression becomes very small at low energy, while the third term becomes small at high energies, so that the product of these two terms is significant only over a very narrow energy range. The product of these two functions over this energy range is called the Gamow peak, and is shown in Figure 16.

The energy range of importance in calculating the reaction rate for the $^{16}O\ (p,\alpha)\ ^{13}N$ reaction is between $E_{P\ LAB} = 6.0$ and 8.0 MeV. The important energy range for the $^{10}B\ (\alpha,n)\ ^{13}N$ reaction is calculated to lie between $E_{\alpha\ LAB} = 0$ and 1.2 MeV, but the large resonance in the cross section near $E_\alpha = 1.5$ MeV shifts this region upwards, because the above discussion assumed that there were no resonances in the cross section.

While the theory of stellar interiors is very complicated, these are a few of the most important definitions and equations, together with a brief discussion of how they apply to the present measurements. More complete discussions may be found in any book on stellar evolution.

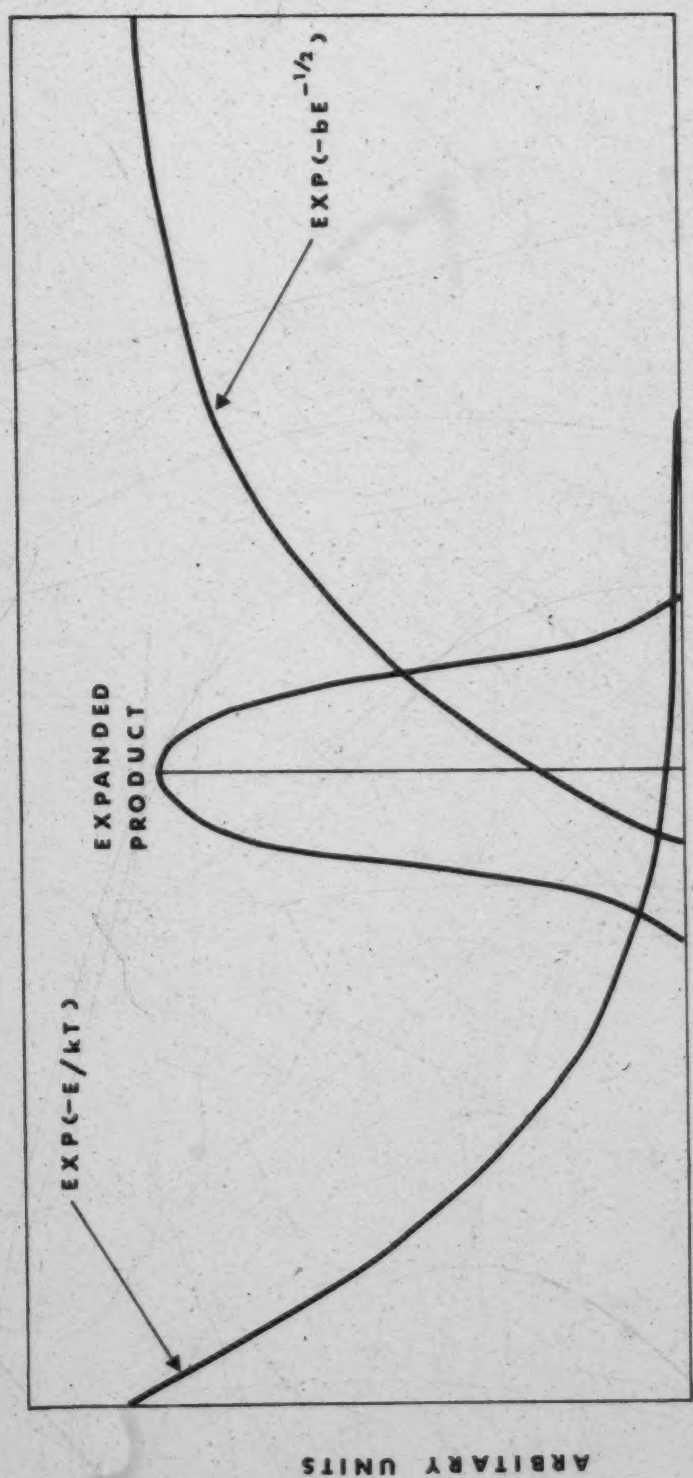

FIGURE 16 SKETCH OF THE GAMOW PEAK

APPENDIX B

CROSS SECTION CALCULATION

The thickness of the targets was calculated from the elastic scattering information using the relation:

$$N_T = \frac{Y}{(\frac{d\sigma}{d\Omega})\ \Delta\Omega\ \ N_P} \qquad \text{B1}$$

where

N_T is the number of target nuclei per cm^2,

Y is the number of counts in the relevant peak of the elastic scattering spectrum per unit time,

$(\frac{d\sigma}{d\Omega})$ is the differential scattering cross section at the angle and energy under consideration,

$\Delta\Omega$ is the solid angle subtended by the detector, and

N_P is the average number of incoming protons (or alphas) incident on the target per unit time.

It should be noted that the number of counts Y was corrected for the dead time of the system.

During the bombardment, the production rate of ^{13}N was given by the relation:

$$\frac{dN}{dt} = N_T\ N_P\ \sigma - \lambda\ N \qquad \text{B2}$$

where $N \equiv$ the number of ^{13}N nuclei present at any instant.

σ = the cross section for the reaction under

consideration at this energy, and,

λ = the decay constant for ^{13}N $((\ln 2)/\tau_{1/2})$.

If N_T and N_P can be assumed constant over the period of the bombardment, then the term N_P N_T σ is a constant. Then this differential equation can easily be integrated from the time the beam is turned on (t = 0) to the time the beam is turned off (t = T) to obtain the following expression for the cross section:

$$\sigma = \frac{A_o}{N_T\ N_P(1- \exp\ (-\lambda T))} \qquad \text{B3}$$

This expression was used to determine the cross section, since all the quantities on the right hand side were known.

It should be noted that by inserting B1 into B3, the factor N_P is eliminated, assuming that the target thickness was determined at the same time that the activation was done (as in ^{16}O (p,α)). However, if these two were not done together (as in ^{10}B (α,n)), then the terms obviously may not be cancelled out.